Chapter

Infrasound Exposure: High-Resolution Measurements Near Wind Power Plants

Huub Bakker, Mariana Alves-Pereira, Richard Mann, Rachel Summers and Philip Dickinson

Abstract

This chapter focuses on infrasonic (≤20 Hz) noise exposure as captured in and around homes located in the vicinity of wind power plants. Despite persistent noise complaints by local residents, no satisfactory acoustical event has yet been identified to justify this troublesome (worldwide) situation. Continuous (days), high-resolution recordings—spectral segmentation of 1/36 of an octave and 1-second temporal increments—have been acquired in many homes across the world revealing the presence of wind turbine acoustic signatures. These consist of trains of airborne pressure pulses, identified in the frequency domain as harmonic series with the fundamental frequency equal to that of the blade-pass frequency of the wind turbine. This report documents three such cases (Portugal and Scotland). The highest peaks of the wind turbine acoustic signature (up to 25 dB over background noise) occurred within the 0.5–5 Hz window which is classically defined as below the human hearing threshold; and yet these 'inaudible' phenomena appear to trigger severe biological reactions. Based on the prominence of the peaks in the harmonic series, a new measure is proposed for use in determining dose–response relationships for infrasonic exposures. This new methodology may be applicable to infrasonic exposures in both environmental and occupational settings.

Keywords: harmonic series, harmonic prominence, wind rose, 1/36-octave bandwidth, time profile, low frequency noise, environmental noise, wind turbines

1. Introduction

Hearing loss, speech intelligibility and noise annoyance are some of the most studied impacts of noise exposures on human health and well-being. A common denominator of these three outcomes is the audibility of the sound. Exposure to loud noise over extended periods of time can cause hearing impairment; noisy environments can interfere with the correct understanding of speech; and certain types of continuous or intermittent sounds can cause people to feel annoyed by noise, which can, in turn, exacerbate underlying disorders or diseases.

There are, however, additional features of sonic environments that are unrelated to the human audibility of sound, but that can also deleteriously affect human health and well-being, specifically, infrasound (≤20 Hz).

1.1 Infrasound and human health: brief overview

With the growing industrialization and mechanization that occurred worldwide in the 1960s, infrasound in the environment began to take its toll on workers and urban citizens. Thus, in 1973, the National Research Council of France organized an International Colloquium entirely dedicated to infrasound [1]. One of the outcomes was the establishment of permissible levels for infrasound exposures in the Russian Federation [2]. **Figure 1** shows the legislated values for the year 2000.

With the introduction of industrial wind turbines (IWT) in mostly rural areas, noise complaints by local residents began to emerge in the media [3, 4, for example] and in scientific journals [5, 6, for example]. And yet, the vast majority of noise measurements performed in and around homes near wind power plants (WPP) showed values well within the established guidelines [7, 8, for example]. This apparently paradoxical situation has even prompted some authors to assume a psychosomatic origin for resident noise complaints [9], or to associate these health complaints with a lack of monetary gain from the WPP [10]. In direct contradiction to the notion of a psychosomatic origin for these noise complaints, are the animal studies showing increased physiological stress when living in the wild, close to WPP [11, for example], or under laboratory conditions, simulating occupational environments [12, 13, for example].

1.2 Frequency-weighting systems, spectral segmentation and temporal resolution as applied to acoustical data acquisition

The ability of the human auditory system to capture sound depends on the combination of the amplitude of the pressure wave (usually evaluated in deciBels, dB, referenced to 20 microPascal), and the frequency (Hz). Different frequencies require different levels of sound pressure in order to be heard. Some decades ago, the International Organization for Standardization (ISO) established a frequency-weighting network that simulated the human hearing threshold and that was specifically focused

No.	Premise	Sound pressure levels, dB, in octaval bands of averaged geometric frequencies, Hz				General sound pressure level dB "Lin"
		2	4	8	16	
1.	Different jobs inside industrial premises and production areas: - Different physical intensity jobs - Different intellectual emotional tension jobs	100 95	95 90	90 85	85 80	100 95
2.	Populated area	90	85	80	75	90
3.	Living and public premises	75	70	65	60	75

Figure 1.
Permissible levels for infrasonic exposures (at 2, 4, 8 and 16 Hz) for two occupational and two environmental settings. Values are provided in dB Linear (no weighting) and, as expected, are lower for public areas than for occupational environments [reproduced from 2].

on preventing hearing loss—the "A" frequency-weighting system [14]. The use of the A-weighting system yields sound pressure levels in the dBA metric.

ISO has also ratified procedures for evaluating infrasound and lower-frequency components: ISO 7196:1995(E) defines the "G" frequency-weighting system as appropriate for quantifying acoustic energy within the range of 0.25–250 Hz [15]. The use of the G-weighting system yields sound pressure levels in the dBG metric. **Figure 2** compares data to which A- and G-weighting have been applied. It also shows the values when no weighting is imposed.

The environment shown in **Figure 2** is within a rural home in the proximity of a WPP, and where residents have noise complaints (see Section 2 below, Home 2). In this 10-minute data segment, the average noise level was less than 30 dBA, well within compliance levels for most rural areas around the world. The G-weighting system, while over-evaluating the sound pressure levels within the range of 10–25 Hz, yielded an average noise level of around 55 dBG. In Japan, for example, the limit for infrasound generated by IWT is 92 dBG [16]. The unweighted capture, which measures the actual levels present in the environment, yielded an average noise level above 60 dB. The highest peaks in this environment, measured without weighting, occurred at frequencies below 8 Hz, i.e., below the defined threshold of human audibility. Taken alone, it would seem that these numerical values are insufficient to adequately characterize the instigator of these residents' noise complaints.

In addition to showing the problematic usage of different frequency-weighting systems, **Figure 2** emphasizes two other aspects of noise measurements: the segmentation of the acoustical spectrum into bands of 1/3 of an octave, and the temporal resolution of 10-minute averages, as per ISO guidelines [14]. As for the spectral segmentation, a higher resolution is technologically possible, but the results are considered mostly academic, since practically all tabulated values related to permissible noise exposure levels use 1/3-octave segmentation.
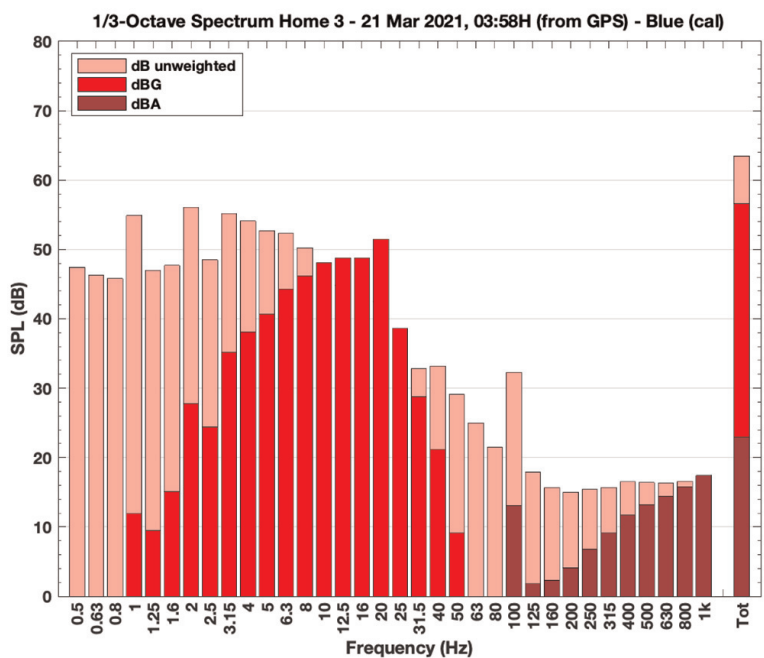

Figure 2.
Comparison of acoustical data acquired with unweighted, G-weighted, and A-weighted systems (10-minute average). Note that between 10 and 25 Hz the G-weighting sound pressure levels are defined to be higher than the unweighted values. (See Section 2 below for detailed methodological capture of this data in Home 2).

1.3 Goal of this report: Going beyond ISO recommendations

Could it be that the spectral segmentation into the 1/3 of an octave and the 10-minute average temporal resolution are too coarse and rudimentary to identify biologically-relevant acoustical phenomena, such as those emanating from WPP?

This report documents the acoustical environments captured in homes located near WPP, using a spectral resolution of 1/36 of an octave, and a temporal resolution of 1-second. Sound pressure levels were analyzed in dB (unweighted).

2. Background and methodology of data collection

Data reported herein were collected in Portugal in Jul-Aug 2020 (Home 1) and in Scotland in Feb-Mar 2021 (Homes 2 and 3), at the invitation of the separate homeowners—usually due to the onset of a pattern of debilitating symptoms which, they claim, only began after WPP became operational in their residential areas [17]. A two-channel sound recording device was placed in and around each home with continuous data acquisition over several days. During the sound recordings, residents were asked to keep a date- and time-logged diary detailing the onset or absence of symptoms, such as sleep disruption. This onset or absence of symptoms could then be compared with changes in the sound recordings that might suggest a causal connection.

2.1 High resolution sound recording

The recording equipment was a SAM Scribe Full Spectrum (FS) system (Soundscape Analytics, Palmerston North, New Zealand), Model Mk1 in Portugal and Mk2 in Scotland [18]. It is a two-channel device with sampling rates up to 44.1 kHz, that is designed to capture recordings of sonic environments with high precision, especially in the infrasonic and low-frequency bands. Data streams are delivered via USB to a Windows notebook computer and stored as uncompressed wav files to a hard disk. GPS information is stored in the files as metadata, which also include a digital signature. Each wav file corresponds to a 10-minute (600-seconds) recording of the sonic environment. The system can accurately record from 0.1–1000 Hz, as per the manufacturer frequency response of the two electret condenser microphones [19].

All measurements reported here cover the range from 0.5–1000 Hz and were captured with a sampling rate of 11.025 kHz. All recordings included a standard reference calibration tone at the start and end, produced with a Type I calibrator (part of the SAM Scribe system) at 1000 Hz/94 dB.

Calibration of the SAM Scribe system rests on 1) the manufacturer's frequency-response curve for the microphone and 2) calibration against a certified Larsen-Davis 831 sound level meter in the range of 6.3–1000 Hz.

2.2 Homes where recordings were captured

2.2.1 Home 1: Portugal (the E. family)

Period of continuous recording: 18 Jul 2020 (00:00)—09 Aug 2020 (10:00). *Microphone location:* At the foot of the bed in master bedroom (ground floor), tripod-mounted 1.5 m above the floor.
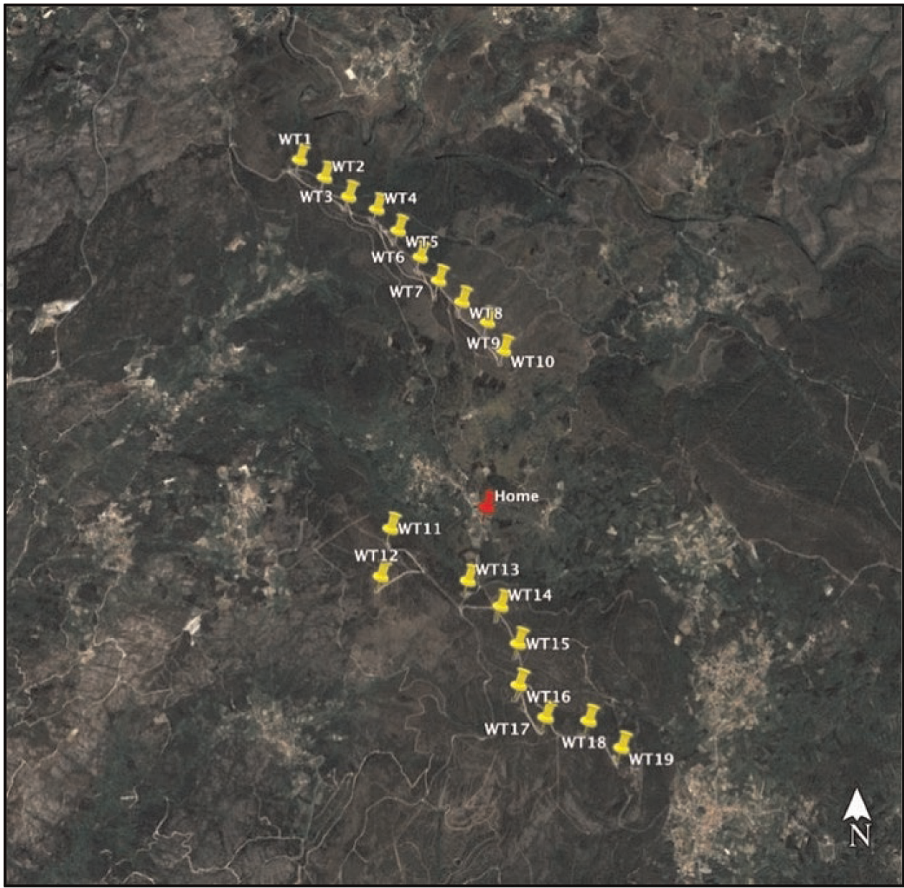
Figure 3.
Relative positions of Home 1 and the 19 industrial wind turbines (labeled WT in the figure) that constitute this wind power plant. (Image adapted from Google Earth).

Figure 3 shows the relative position of Home 1 and the WPP (19 Senvion MM92 turbines of 2 MW each, with blade length 45.2 m). The closest IWTs to the home are numbers 11, 12, 13 and 14, at 843 m, 1085 m, 648 m, and 844 m, respectively. IWT1 and IWT19 are the furthest away, at a distance of 3422 m and 2282 m, respectively.

The E. family—Mr. E. (age 63) and Mrs. E. (age 64)—have lived amid these 19 IWT since 2016. Their health deterioration has been documented by neurological medical reports.

2.2.2 Home 2: Scotland (the P. family)

Period of continuous recording: 24 Feb 2021 (17:30)—07 Mar 2021 (00:00).
Microphone location: Beside the head of the bed in an upstairs bedroom with a dormer, tripod-mounted 1.5 m above the floor.

Mrs. P documented some of her symptoms from Jul 2019 to Mar 2020. **Table 1** shows a 6-month sample (Jul–Dec 2019).

2.2.3 Home 3 – Scotland (The J. Family)

Period of continuous recording: 20 Mar 2021 (16:20)—27 Mar 2021 (18:40).
Microphone location: Middle of attic bedroom, tripod-mounted 1.5 m above the floor.

Symptom	Dates on which symptom was reported
Nausea	6 Jul, 3 Aug, 18 Aug, 12 Oct, 20 Oct, 4 Nov, 6–7 Nov, 10 Nov
Dizziness	7 Jul, 3 Aug, 13–14 Sep, 20–21 Sep, 26 Sep, 28 Sep, 24 Nov, 14–16
Pain in ears	5–9 Jul, 15 Jul, 18 Jul, 22 Jul, 26 Jul, 31 ul, 1 Aug, 3 Aug, 9–12 Aug, 21 Aug, 23 Aug, 13–14 Sep, 2 Oct, 4–5 Oct, 10 Oct, 17 Nov, 22 Dec, 27 Dec, 30 Dec
Sleep disturbance	2 Jul, 4 Jul, 14 Jul, 18 Jul, 22 Jul, 24 Jul, 13 Aug, 25 Aug, 13 Sep, 20 Sep, 12 Oct, 15 Oct, 3–5 Nov, 17 Nov, 23 Nov

Table 1.
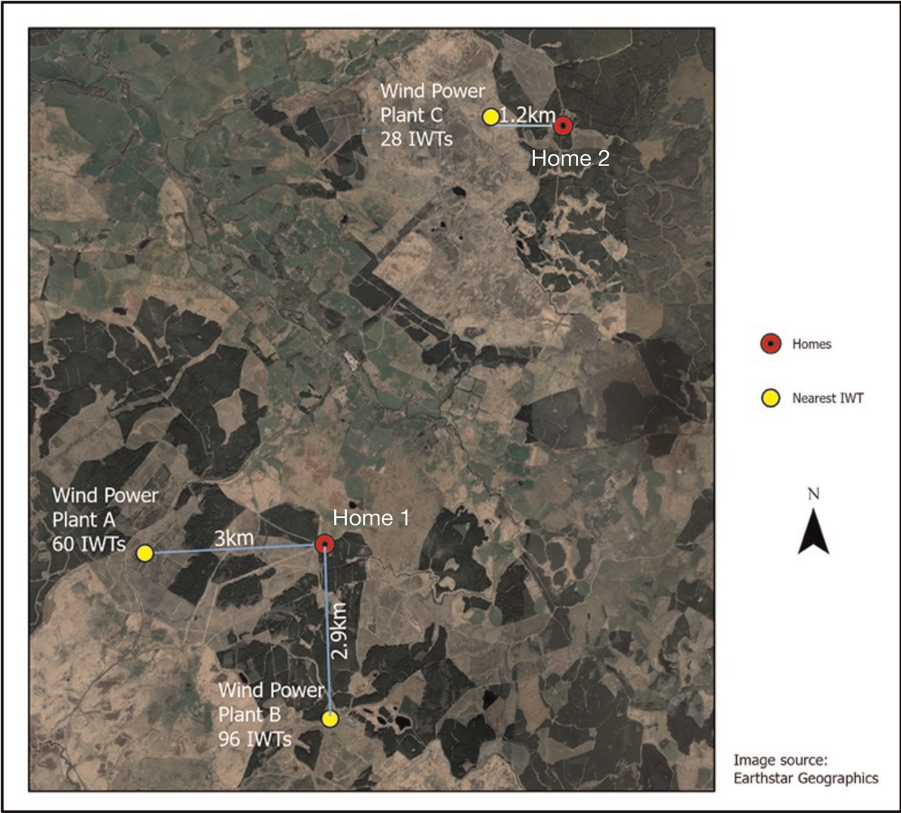*Six-month sample of some of the symptoms documented by Mrs. P.*

Figure 4.
Relative positions of Home 2 and Home 3 and the closest industrial wind turbines of wind power plants A, B and C.

Figure 4 shows the relative positions between Homes 2 and 3, and the three WPP located in the vicinity.

WPP A has 60 Gamesa G80/2000 turbines of 2 MW each, with blade diameters of 80 m. It is located 4.6 km to the west of Home 2 and 14.5 km to the southwest of Home 3. It has been operational since 2011.

WPP B has 96 Gamesa G114/2500 turbines of 2.5 MW each, with blade diameters of 114 m. It is located approximately 2.9 km to the south of Home 2 and 13.1 km to the south of Home 3. It has been operational since 2007.

WPP C has 28 Gamesa 87/2000 of 2 MW each, with blade diameters of 87 m. It is located approximately 9.5 km to the north of Home 2 and 2.1 km to the southwest of Home 3. It has been operational since 2011.

2.3 Wind data

Information on wind speed and direction was retrieved for the entire period during which recordings were made.

In Portugal, data was obtained from the Portuguese Institute of Sea and Atmosphere (IPMA [20]). Data points were requested in 10-minute increments, from three distinct meteorological stations: at 58 km (altitude above sea level: 995 m), 12.5 km (altitude above sea level: 642 m) and 52.7 km (altitude above sea level: 558 m) away from the E. family home (altitude above sea level: 850 m). In Scotland, weather data was obtained from the British National Weather Institute via the Open Weather service [21] in one-hour intervals. The location for which weather data was obtained was 3.5 km away from Home 2 and 7.8 km from Home 3. Wind data was time-matched to the GPS time-stamped acoustical recordings.

3. Results

3.1 Home 1: Diary

The E. family kept a diary from 13 July through 31 July, 2020.

On 29 July at 04:00, the family's sleep had been disrupted for several hours and Mr. E. felt so unwell that he was compelled to take medication (benzodiazepine) (*'Severe' episode*). By comparison, on the morning of 22 July, Mr. and Mrs. E. slept uninterruptedly until 07:00 (*'Peaceful' episode*).

Priority was therefore given to the analysis of the period between 03:00 and 06:00 (eighteen 10-minute recordings) on both these days, the choice of identical diurnal periods helping to alleviate any extraneous differences between the two mornings.

3.2 Home 1: At 03:20 on the morning of the 'severe' episode (29 Jul, 2020)

Figure 5 shows the results of the sound data acquired between 03:20 and 03:30, on the morning of 29 July, when the E. family's sleep was disrupted and Mr. E. felt the need to self-medicate.
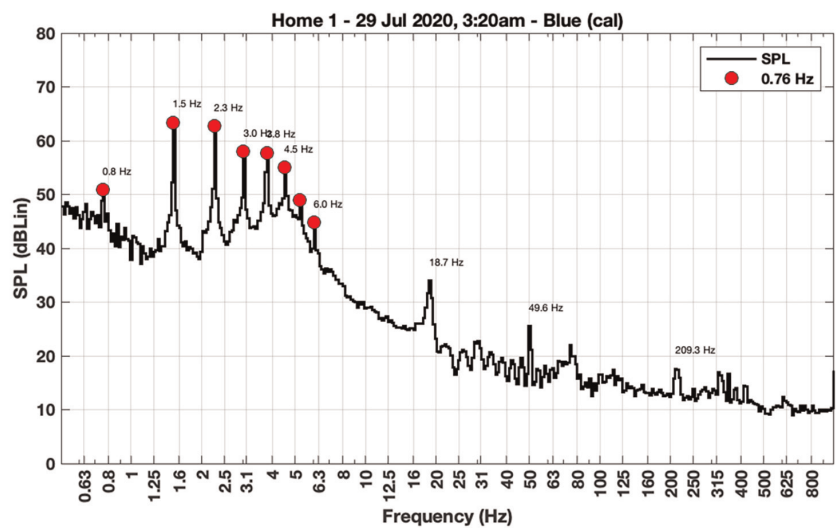
Figure 5A shows a sonogram reflecting the acoustic environment inside the bedroom over a 10-minute period (600 seconds), with 1/36th-octave-band resolution (vertical axis) and 1-second temporal resolution (horizontal axis). The sound pressure level at each frequency and at each second in time, is indicated in the color-coded scale on the right (measured in dB). The yellow color of the straight, horizontal lines visible across the image at 1.5 Hz, 2.3 Hz, 3.0 Hz, and 3.8 Hz reflect the large amount of acoustic energy (50–60 dB) present at these frequencies. Additionally, the lack of discontinuities in these lines indicate that the phenomena were continuously present during the entire 600 seconds.

Figure 5B shows the same numerical data as in **Figure 5A**, but as a frequency spectrum. A series of peaks is readily identifiable, occurring at the same frequencies as the continuous, horizontal lines seen in the sonogram (**Figure 5A**). The mathematical relationship between the frequencies of each peak (red dots) constitutes a harmonic series with a fundamental frequency of 0.76 Hz (0.8 Hz in the figure).

In all 18 recordings (from 03:00 to 06:00, 29 Jul), the sonograms presented similar, continuous horizontal lines and, in all corresponding spectrograms, the same harmonic series (fundamental at 0.76 Hz) was visible. The blade-pass frequency of the IWT
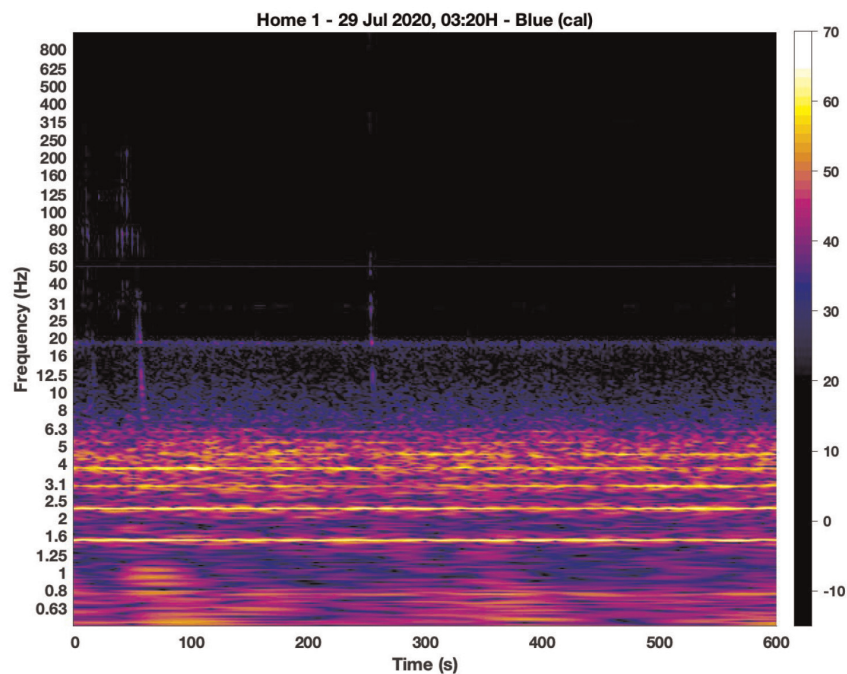
(A)

(B)

Figure 5.
(A) Sonogram *showing the sonic environment inside the master bedroom of home 1 (on 29th Jul when sleep was disrupted and medication was required) over a 10-minute period (600 seconds), with 1/36-octave band resolution ('frequency' on vertical axis) and 1-second temporal resolution ('time' on horizontal axis). The color-coded scale on the right measures sound pressure level in (unweighted) dB. Continuous (over the entire 600-second interval), horizontal lines cross the image at 1.5 Hz, 2.3 Hz, 3.0 Hz, and 3.8 Hz with a pressure level of 50–60 dB.*
(B) Spectrogram *in the form of a frequency distribution, constructed with the same numerical data as in* **Figure 5A**. *A harmonic series is identified when the frequencies of each peak (red dots) are multiples of the fundamental frequency of 0.76 Hz (0.8 Hz in the figure).*

installed around the home of family E. is 0.75 Hz. The harmonic series identified in Home 1 is the acoustic signature that emanates from these machines, and that reflects the airborne propagation of a pulsed, pressure wave generated by rotating IWT blades. This IWT acoustic signature occurs below the threshold of human audibility.

3.3 Home 1: At 04:00 on the morning of the 'peaceful' episode (22 Jul, 2020)

In **Figure 6**, the sonic environment in the master bedroom of family E. is shown, as captured between 04:00 and 04:10, on the morning of 22 July, when the E. family slept peacefully. The lack of continuous, horizontal lines throughout the sonogram (**Figure 6A**) is notable, as is the absence of regular peaks in the corresponding
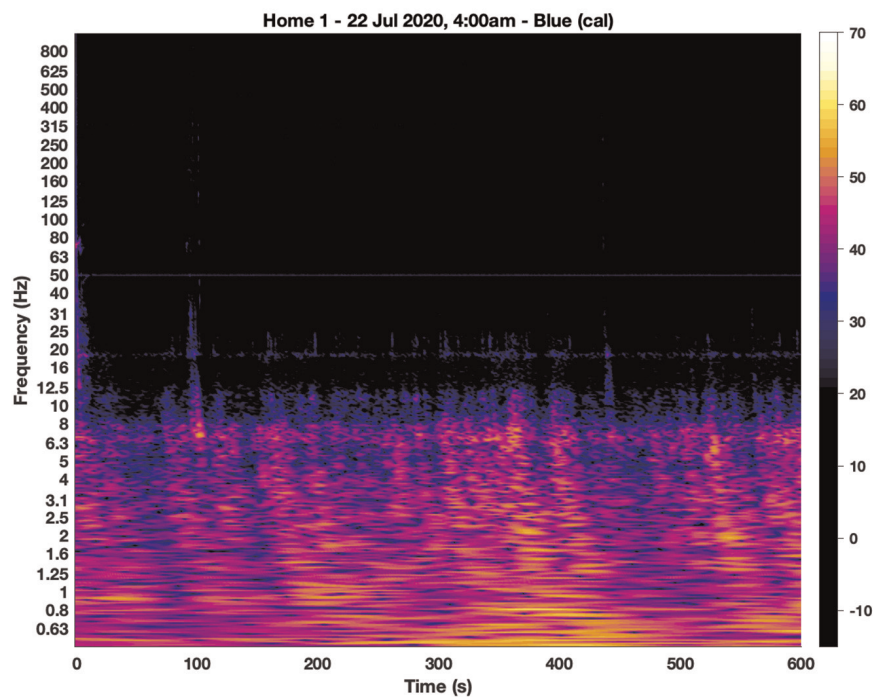
(A)
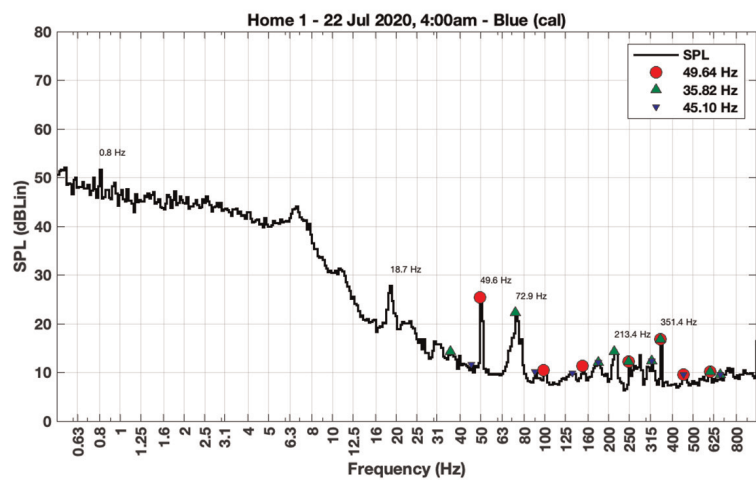
(B)

Figure 6.
(A) Sonogram *showing the sonic environment inside the master bedroom of Home 1 (on 22nd Jul when no sleep disruption occurred) over a period of 600 seconds—With 1/36-octave band resolution, 1-second temporal resolution—and pressure levels in dB as indicated by the color-coded scale. The triangular, pink shapes that span various frequencies are due to blowing wind, and do not exceed 50 dB. Continuous, horizontal lines as observed in* **Figure 5A** *are absent. (B)* Spectrogram *without any regular, large peaks of acoustic energy in the infrasonic range. Harmonic series, as related to IWT acoustic signatures, are absent.*

spectrogram (**Figure 6B**). The triangular, pink shapes that span various frequencies in the sonogram are due to blowing wind, and do not exceed 50 dB. In all 18 recordings (from 03:00 to 06:00, 22 Jul), no IWT acoustic signature was identified.

3.4 Homes 2 and 3

Regrettably, the residents of these Homes were not sufficiently assiduous with their diary entries so that health-related information could be compared with simultaneous recordings.

Homes 2 and 3 have three different models of IWT among the 3 WPP located in their vicinity, as opposed to Home 1 that only had one type. For asynchronous (constant with varying wind speeds) IWTs, each model will have its own blade-pass frequency and, therefore, their acoustic signatures will be different.

Figure 7 shows the sonogram and spectrogram of the sonic environment captured in the attic bedroom in Home 3. The very clean and continuous horizontal lines that extend throughout the 600-second recording (**Figure 7A**) reflect the existence of a prominent IWT acoustic signature. This is confirmed by the sequence of peaks that constitute the harmonic series, as can be clearly identified in the corresponding spectrogram (**Figure 7B**). The two harmonic series (i.e., IWT acoustic signatures) identified in Home 3 are also present in Home 2, as can be seen in the spectrogram in **Figure 8**.

Figures 7B and **8** show very similar examples of dominant IWT acoustic signatures. The harmonic analysis highlights a harmonic series with a fundamental frequency of 1 Hz (0.99 Hz in the figures) and at least the first 19 harmonics. The Gamesa 80 and 87 IWT models have a blade-pass frequency of 1 Hz. A second harmonic series is identified with a fundamental frequency of 0.67 Hz. The blade-pass frequency for the Gamesa 114 model is 0.67 Hz. A separate harmonic series begins at 20 Hz from an unknown source, possibly the IWT gearboxes.

4. Discussion

4.1 Sleep disruption and the prominence of harmonic peaks

The harmonic series observed in all 18 samples of the 'severe' episode, and that were absent in all 18 samples of the 'peaceful' episode, is recognized as the IWT acoustic signature with a blade-pass frequency of 0.75 Hz. The acoustic signature generated by an IWT is a train of pressure pulses, with a period equal to the reciprocal of the blade-pass frequency of the IWT. It presents as a harmonic series of peaks in the infrasonic region of a spectrogram, visible in **Figures 5B, 7B** and **8**, while absent from **Figure 6B**. In the sonograms, the IWT acoustic signature is present as continuous horizontal lines, as seen in **Figures 5A**, and **7A**, while absent from **Figure 6A**.

This new, high-resolution methodology for assessing infrasonic environments is analogous to transitioning from a magnifying glass to a microscope. Previously undetected acoustic events are now identifiable and, even, quantifiable (see Sections 5.2 and 5.3 below). What was undetectable—and thus assumed to be non-existent, presumably justifying a psychosomatic origin for resident complaints—using the classical noise assessment methodologies (1/3-octave band segmentation in 10-minute averages and with sound pressure levels measured in dBA or dBG), became visible with high-resolution observations.
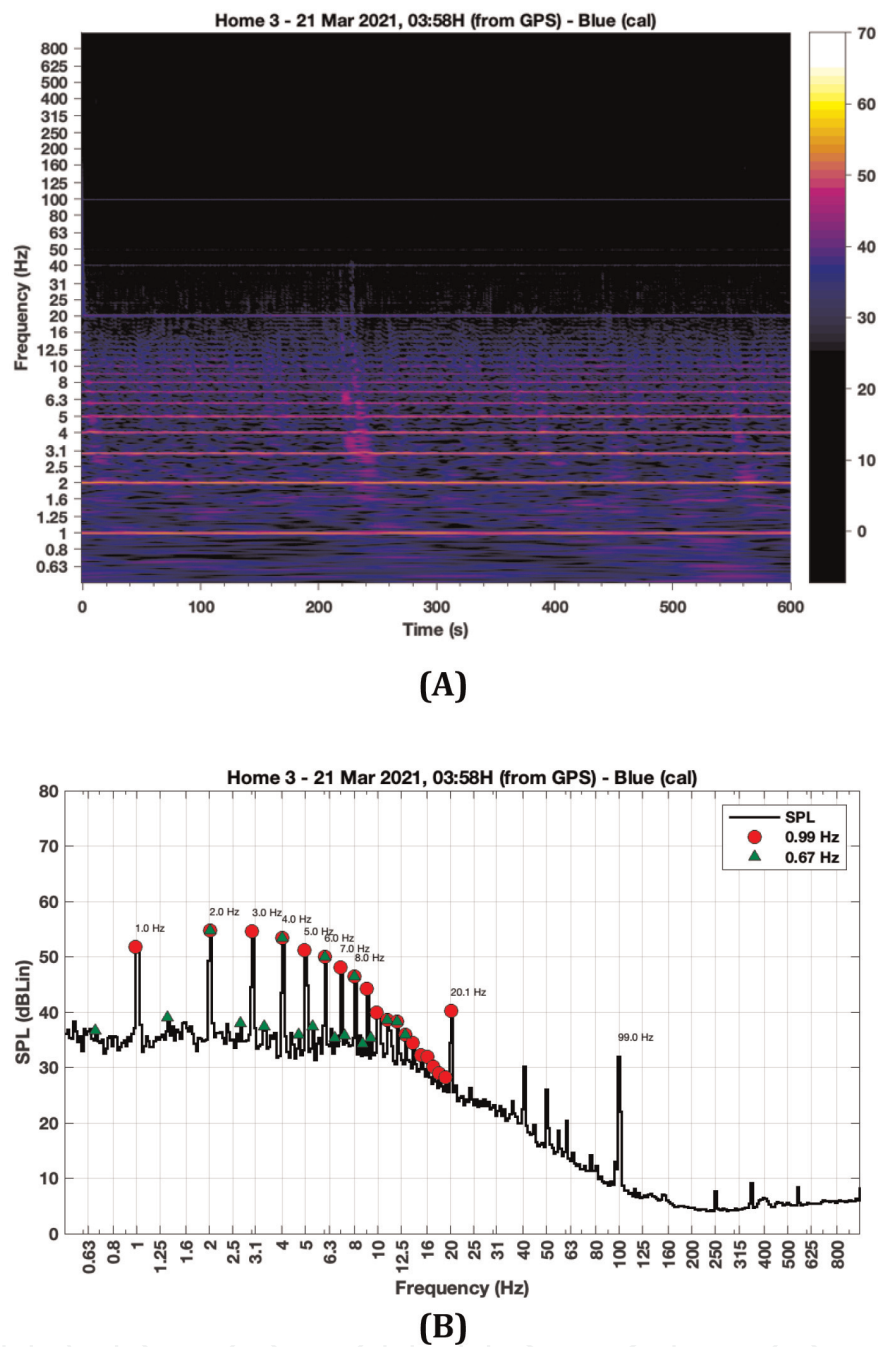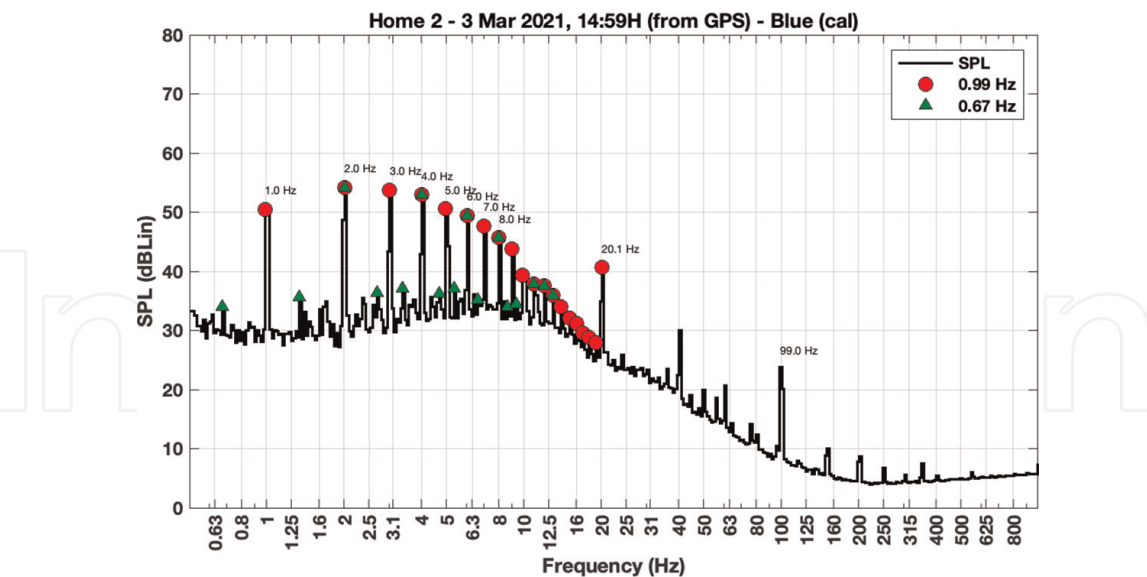
(A)

(B)

Figure 7.
(A) Sonogram *showing the sonic environment inside the attic bedroom of Home 3 over a period of 600 seconds, with 1/36-octave band resolution, 1-second temporal resolution, and pressure levels in dB, as indicated by the color-coded scale. Continuous, horizontal lines are readily observable at frequencies below the threshold of audibility, and that reflect the existence of IWT acoustic signatures. (B)* Spectrogram *showing the two most prominent harmonic series, with fundamental frequencies at 0.67 Hz and 0.99 Hz, reflecting IWT acoustic signatures from different IWT models, with different blade-pass frequencies.*

Despite being at frequencies and sound pressure levels that are classically considered as 'below the human hearing threshold,' a very clear correlation has been shown between the existence of these peaks in the frequency spectra and disruption of the normal biological function—sleep disruption followed by the need for self-medication with benzodiazepines. Nevertheless, while the correlation is very clear, the confidence of the correlation is reduced by the relatively small timeframe. Improved confidence
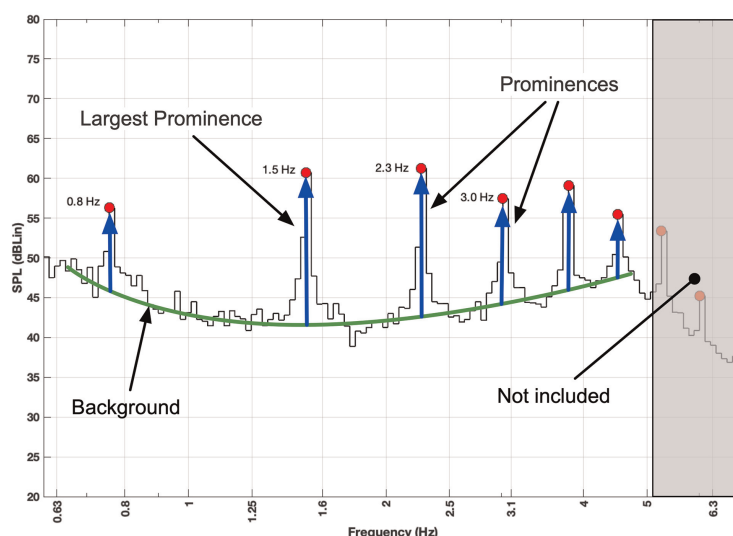
Figure 8.
Spectrogram *showing the sonic environment inside the upstairs bedroom of Home 2, over a period of 600 seconds, with 1/36-octave band resolution and 1-second temporal resolution. Two of the most prominent harmonic series are readily identifiable, with fundamental frequencies at 0.67 Hz and 0.99 Hz, reflecting IWT acoustic signatures from different IWT models, with different blade-pass frequencies.*

can only come from more work to extend the use of this measure to many other cases (an ongoing endeavor by these authors).

The question as to how these infrasonic acoustic events can cause the biological disruption is still unclear. Studies by German scientists, however, using functional magnetic resonance imaging—while exposing subjects to infrasound—may have uncovered a significant clue: in addition to activating the classically identified auditory pathways, infrasonic stimuli also activate regions of the brain that are considered responsible for emotional and autonomic responses [22].

4.2 Prominence of the harmonic peaks—A new metric?

The prominence of these harmonic peaks above the background noise appears to be highly relevant for health-related issues. **Figure 9** depicts a harmonic series as identified in an IWT acoustic signature, an airborne train of pulses occurring within the 0.5–5 Hz window. Note that the persistent or continuous existence of this type of harmonic series ties this acoustic event to human-made sources because the manifestations of such harmonic series from natural sources are exceedingly rare. There is no established methodology to quantify the prominence of these peaks.

A new metric is herein suggested; one that may more accurately provide a measure of the "dose" of this pulsed agent of disease. We have called this measure the *Harmonic Prominence*, H_p, defined as the largest prominence of any harmonic frequency of any harmonic series, within the 0.5–5-hertz frequency window. In **Figure 9**, H_p = 17 dB, at 1.5 Hz. In the specific case of IWT, only harmonic series with a fundamental frequency equal to the IWT blade-pass frequency are considered. In the specific case of the data acquisition methodology detailed above, the highest prominence of the harmonic series is determined in temporal segments of 600-seconds.

There are a variety of mathematical definitions, methodologies and software packages associated with quantifying peak prominence above background, for almost any and all types of wave phenomena. These authors have adhered to the formal

Figure 9.
Determination of prominence levels based on 1/36-octave frequency bands. The largest prominence, H_p (see text), in this series is approximately 17 dB over background. (Numerical data for this figure were obtained in Home 1, during the 'severe' episode).

definition of prominence in a frequency spectrogram as established by MATLAB which has a robust definition of prominence in terms of the peak height and the local background level [23].

The H_p parameter does not measure the total energy of the pulses in the pulse train that emanates from IWT. This energy is spread out over all the harmonic components of the pulses—the peaks in the spectrogram—whereas the measure only looks at the peak with the largest prominence. Therefore, H_p cannot be considered as an energy measure.

Another approach would be to look in the time domain, rather than in the frequency domain. Here a measure such as the crest factor could be used to gain a measure of the 'peakiness' of the pulses, using their total energy. These additional avenues of research are undergoing further scrutiny by these authors and their colleagues [17].

4.3 Day-time plots—Evaluation of long-term infrasound exposures

The H_p parameter can provide health scientists with a rudimentary indicator of the largest prominence above background that exists within a 10-minute measurement. When continuous measurements are maintained over several days (or weeks), a clearer picture regarding the long-term variation of exposure to these trains of pulses is revealed.

Figure 10 shows a Day-Time plot for the data collected in Home 1, 18 Jul-09 Aug, 2020. Here H_p is plotted as a surface with the date as the abscissa and the time of day as the ordinate. For each 24-hour period, there are 144 ten-minute samples. The values of H_p were determined for each 10-minute sample, and then binned (scale: <5 dB, 5–10 dB, 10–15 dB, 15–20 dB, 20–25 dB and > 25 dB), as reflected by the color-coded scale in **Figure 10**.

Similar day-time plots were constructed for Homes 2 and 3, as shown in **Figures 11** and **12**, respectively. While these types of plots are informative as to the time and
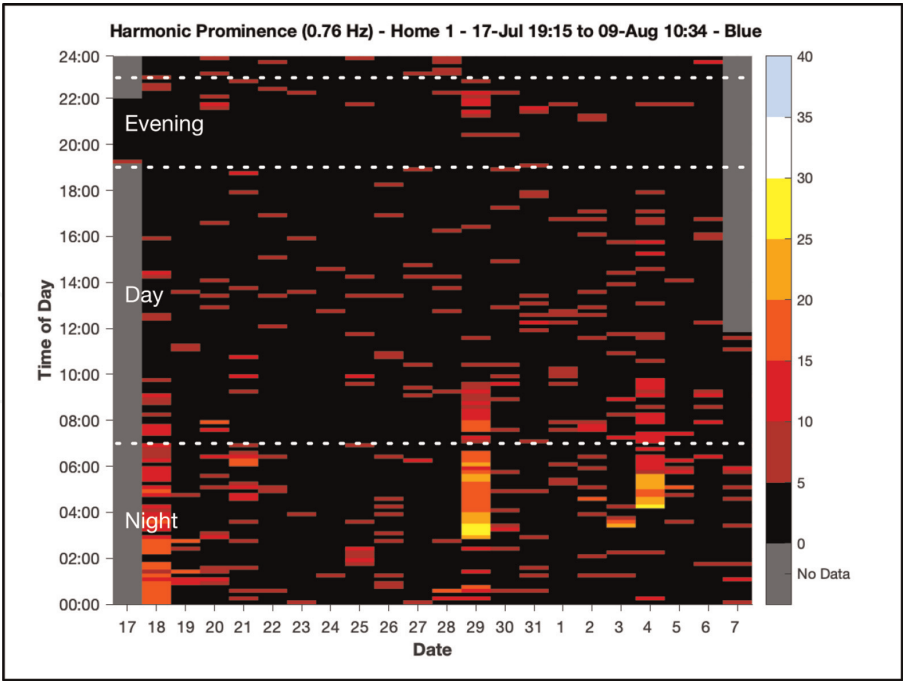
13

Figure 10.
Day-time plot for Home 1. *The 'severe' episode took place on 29th Jul, while the 'peaceful' episode took place on 22 Jul. The nights of 18 Jul and 4 Aug also show the presence of prominences. The 'peaceful' morning (22 Jul) has only one 10-minute sample with a significant H_p level. The following two mornings also appear to have no significant H_p samples but were not noted in the residents' diary as either peaceful or disturbed. The 'severe' morning (29 Jul), from 3 am until about 9 am shows up in stark contrast to the other mornings, indicating not only that the H_p levels were high but also that they were the highest in the entire length of the recording. The night of 4 Aug also shows an interval of 10-minute samples with severe H_p levels. Since the residents' diary stops on 31 Jul their experience on this day was not recorded. Finally, the night of 18 Jul shows elevated H_p levels from midnight onwards, although these did not reach the same levels as for 29 Jul or 4 Aug. The Es' diary entry for 18 Jul at 04:00 indicated that the "noise was unbearable" and "sounded like a derailing train."*

duration that people are exposed to higher or lower levels of H_p, it is still important to view the sonograms to get a true understanding of the nature of the sonic environment at that point in time. For example, it is not possible from this graph alone to determine if the lower H_p levels seen in Home 2 on the morning of the 27th (**Figure 11**) are caused by the presence of a higher background noise level or whether the levels of H_p were actually diminished.

Note that not all the 10-minute intervals where the H_p is shown as 0 (black) are, in fact, 0. Impulsive sound—caused by such events as people walking over a floor or a door closing—can contaminate an entire 10-minute recording since the impulse is spread over longer and longer time intervals as the frequency of the 1/36-octave bands decrease.

To use the H_p measure as part of a dose–response metric, the simplest method would be to integrate it over time, i.e., multiply each value by 10 minutes and sum for a metric in decibel-minutes. Long-term exposure might be measured in decibel-years. Future research might even develop infrasound dosimeters for workers, similar to those used for radiation exposures.

Comparing the infrasonic environment in Home 1 with those encountered in Homes 2 and 3, a major difference becomes obvious: in the latter two homes, periods of respite (black areas in the day-time plots) are almost non-existent. Periods of respite are understood as biological recovery times, during which the agent of disease is not present and physiological cellular repair can be undertaken unimpeded by the acoustic aggressor. In Home 1 there is the possibility of comparison between the
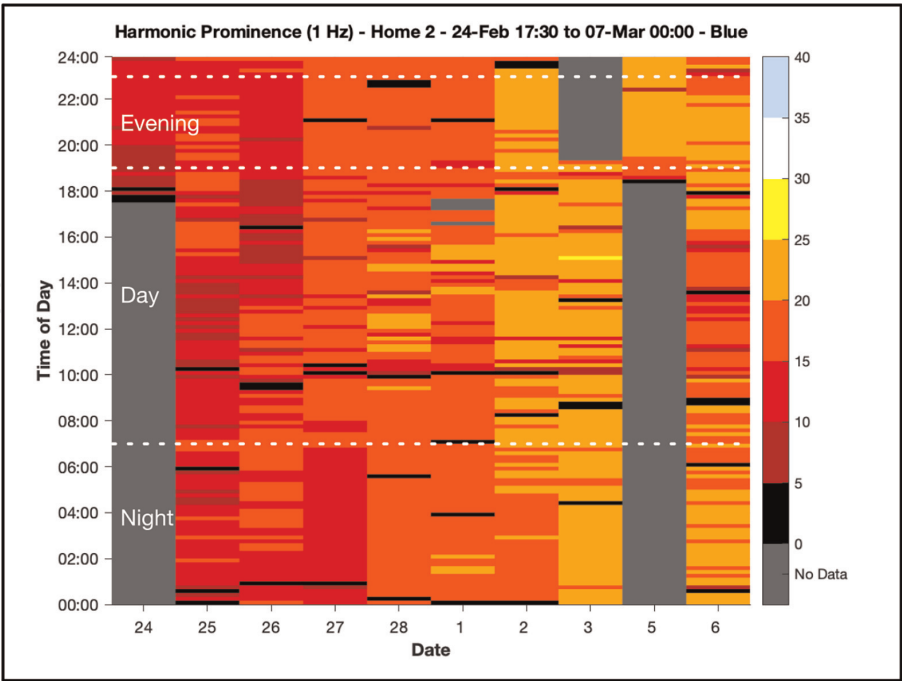
Figure 11.
Day-time plot for Home 2. *A visual inspection shows that the H_p was most dominant from the 2nd through the morning of the 6th reaching its highest value at around 3 pm on the 3rd, with H_p between 25 and 30 dB above background.*
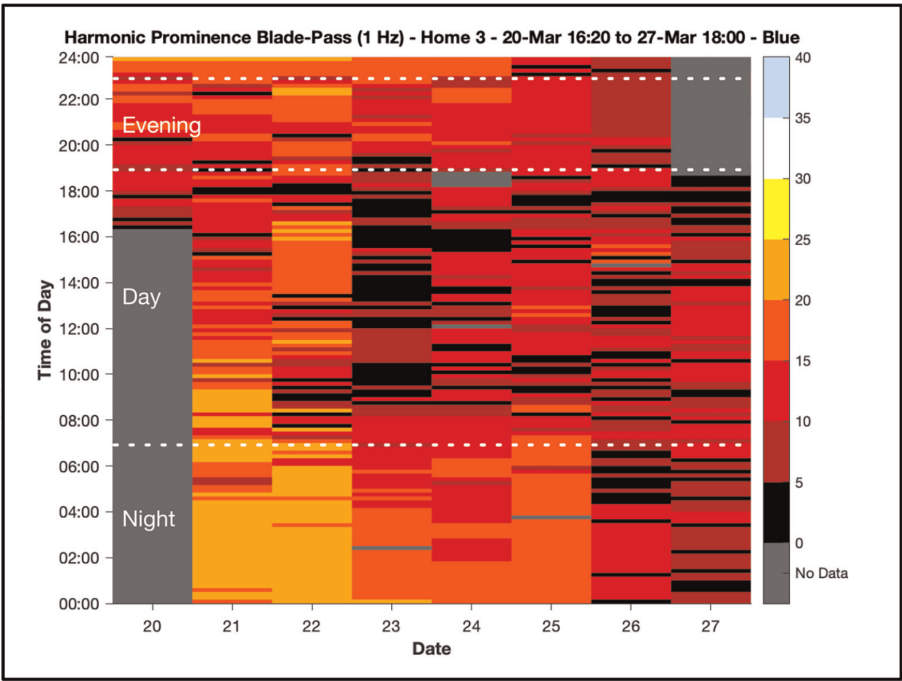

Figure 12.
Day-time plot for Home 3. *The most dominant episodes, i.e., highest level of H_p, were at night. The mornings of the 21st and 22nd registered the strongest H_p (20–25 dB), while the morning of the 27th presented with the weakest.*

periods of time when the IWT acoustic signature is present and when it is absent. Clearly, this is a much more difficult proposition in Homes 2 and 3, where the H_p level indicates that IWT acoustic signatures are almost always present, to a greater or lesser extent (color-coded scale).

4.4 Harmonic prominences wind roses

Airborne sound propagation is affected by wind and weather conditions. In addition to the obvious fact that wind 'carries sound,' thus reducing attenuation downwind, other atmospheric properties can greatly alter both the propagation and attenuation of sound. For instance, increasing humidity will improve propagation, while atmospheric inversion layers can create 'dead zones' where sounds will not be heard despite proximity to the source. Beyond these effects, the propagation and attenuation of infrasound differs in some important respects from sound at higher frequencies. While higher-frequency sound diminishes by 6 dB per doubling of distance—the inverse-square law—infrasound only diminishes by 3 dB. Infrasound is also more prone to refraction around large objects such as hills and to being funneled down valleys.

A data fusion of meteorological data (wind direction) and acoustic data (H_p) can provide insight into these weather- and terrain-induced differences that can significantly influence H_p levels. A *harmonic prominence wind rose*, which takes its inspiration from the common wind rose, is the nomenclature given to this data fusion. An example can be seen in **Figure 13**, reflecting data obtained in Home 1.

The H_p wind rose is a stacked, frequency histogram plotted in polar coordinates. It shows the number of 10-minute samples with an H_p in each dB-level bin in the direction of the then-prevailing wind. Each bin is identified by a color and the number of samples is indicated by the length of each segment in the radial direction. This provides important information if, for instance, the strongest levels of H_p align with a given wind direction.

The closest national meteorological stations must be used to provide wind data if a certified weather station is not available at the site of the sound recordings. This may be problematic since many weather services do not provide data at the closest weather
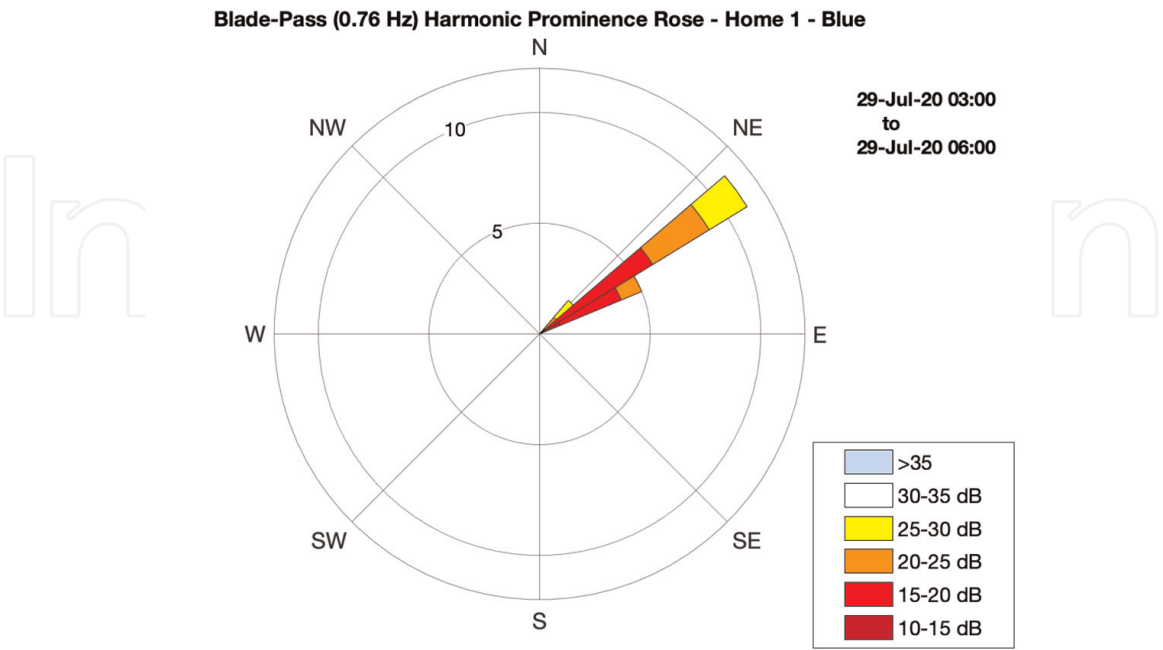

Figure 13.
Harmonic prominence wind rose for Home 1. *Data refers to the 18 samples examined during the 'severe' episode. The highest Hp levels (yellow) were registered when wind was from the north-eastern quadrant. (Wind data from weather station located 12.5 km from Home 1).*

station but rather synthesized weather information, using their proprietary weather models. The wind direction provided is, therefore, not necessarily the same as at the recording site. Moreover, the wind direction at the hub-height of the IWTs may not be the same as at the height of the weather station or the home. The wind direction cannot, therefore, be said to indicate the direction of the source of the IWT acoustic signature in relation to the home.

While the wind direction can provide some understanding, the windspeed may also have a tale to tell. This leads to H_p wind roses plotted for data within wind-speed ranges. Examples are shown in **Figures 14** and **15** for three ranges. The left graph is a H_p wind rose for all 10-minute periods in the recording interval when the wind was between 0 and 10 km/h, the middle graph is for wind speeds of 10–30 km/h and the right graph is for wind speeds of 30–60 km/h.

The fact that the multi-day recording in Home 3 does not include any wind from the eastern half of the compass emphasizes the fact that a reasonable sampling of wind conditions will involve recordings from throughout the year to cover all seasons.
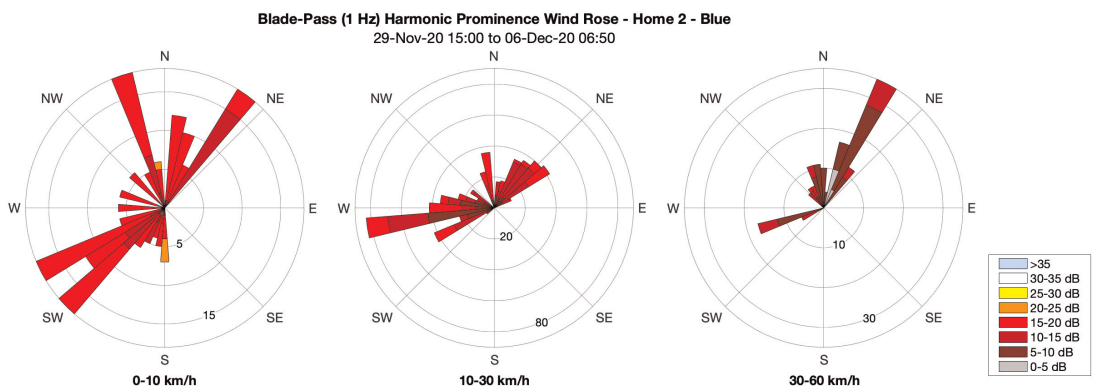
Figure 14.
Harmonic prominence wind roses for three wind-speed ranges for Home 2. *The strongest H_p is at the lowest windspeed, and this is most consistently dominant when the wind is between southwest and north-northeast; i.e., the sectors of the wind rose in these directions are almost entirely made up of 10-minute intervals where the H_p was between 15 and 20 dB (red). By comparison, where the wind was from the northeast, only about 15% of the sound files have this level. At the highest windspeeds, no instances of 15–20 dB H_p can be seen.*
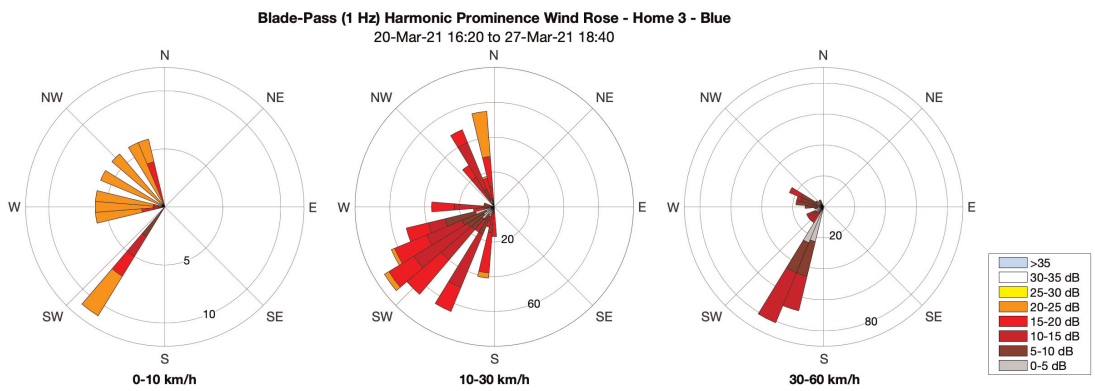

Figure 15.
Harmonic prominence wind roses for three wind-speed ranges for Home 3. *The strongest H_p is at the lowest windspeed and this is most consistently dominant when the wind is from the west through to northwest. That is, the sectors of the wind rose in these directions are almost entirely made up of 10-minute intervals where the H_p was between 20 and 25 dB (orange). By comparison, where the wind was from the southwest, only about 1/3 of the sound files have this level. At the highest windspeeds, no instances of even 15–20 dB H_p can be seen.*

The inverse dependence of H_p on wind speed is because the wind noise increases with wind speed, thus increasing the levels of background noise—including in the infrasound region. The sound pressure levels of the IWT pulses, however, remain constant. Thus, H_p will have lower values (see **Figure 9**). The unanswered question is whether the human brain processes the information of the IWT acoustic signatures when these appear obscured by, or embedded in, the increased background noise, as measured by a machine.

4.5 The position of other authors

In this type of scientific endeavor, it is normally expected that the work of other authors also be presented to form a context and allow a comparative analysis of results obtained and/or of the methodologies used. Regrettably, most, if not all, papers on infrasound are conducted with a ⅓–octave resolution, which immediately precludes any data comparison with that presented here. Due to a variety of conditioning factors that have been in place for decades, sound level meters readily available on the market do not possess the technical capabilities for this type of data acquisition and subsequent analyses. Simultaneously, many of the health-related aspects that are studied within the context of IWT are restricted to measures of "annoyance" (a non-clinical and highly subjective parameter) or to the audibility of the sound, neither of which are very relevant to the results presented here.

In 2018, the World Health Organization (WHO) published a document titled: *Environmental Noise Guidelines for the European Region* [24]. The word "infrasound" has one single entry, on page 85, under the section heading *Wind turbine noise*:

> *"Wind turbines can generate infrasound or lower frequencies of sound than traffic sources. However, few studies relating exposure to such noise from wind turbines to health effects are available. It is also unknown whether lower frequencies of sound generated outdoors are audible indoors, particularly when windows are closed."*

These and other statements reflect a profound misunderstanding of the importance of the time-profile of an exposure to sound as it relates to biological responses (e.g., traffic does not produce harmonic peaks with a one-second pulse rate). However, in defense of this position taken by the WHO, it must be acknowledged that the methodologies it uses for assessing sound necessarily preclude the observation and identification of harmonic series associated with IWT. The suggestion that the audibility of infrasound levels (in itself, an oxymoron by classical definitions) can be mitigated by closed windows clearly indicates a profound lack of knowledge on the physical attributes of propagating airborne pressure waves within the infrasonic range [25–27].

5. Conclusions

This chapter provides a different approach to the measurement and analysis of infrasound in and around homes located in the proximity of wind power plants. Examples show how using higher temporal- and spectral-resolutions (1 second and 1/36 of an octave), and without any frequency weighting, can reveal acoustical features in the infrasonic range that may indicate a causal relationship with self-reported medical symptoms. This possibility is usually considered non-existent since the infrasonic range is generally viewed as inaudible, and thus innocuous, to humans. The

suggestion therefore arises that current noise protection procedures are insufficient to protect public and occupational health. The approach used by these authors offers a more solid framework with which to pursue the establishment of dose–response relationships for infrasonic exposures. Future studies are being extended into noisy occupational environments and different environmental settings where wind power is not the acoustic source.

Acknowledgements

Conflicts of interest

HHCB developed software for capturing and analyzing the sound files for the SAM system, no financial interest. MAP no conflict. RM no conflict. RS contributed to the development of the SAM system, no financial interest. PD no conflict.

Author details

Huub Bakker[1], Mariana Alves-Pereira[2]*, Richard Mann[3], Rachel Summers[1] and Philip Dickinson[1]

1 International Acoustics Research Organization (IARO), Palmerston North, New Zealand

2 Lusófona University, Lisbon, Portugal

3 University of Waterloo, Ontario, Canada

*Address all correspondence to: m.alvespereira@gmail.com

IntechOpen

References

[1] Pimorov L, editor. Les Infra-Sons. France: CNRS Publishing; 1974

[2] Stepanov V. Biological Effects of Low Frequency Acoustic Oscillations and Their Hygienic Regulation. Moscow: State Research Center of the Russian Federation; 2000

[3] Kaeding EF. The curse of repowering – A long descent. Die Tageszeitung. 2014. [In German] https://www.taz.de/Archiv-Suche/!5032786&s=hogeveen/

[4] Wetzel D. [Energy Danish Debate - Does the infrasound of wind turbines make you sick?]. Die Welt. 2015. [In German] https://www.welt.de/wirtschaft/energie/article137970641/Macht-der-Infraschall-von-Windkraftanlagen-krank.html

[5] Dumbrille A, McMurtry RY, Krogh CM. Wind turbines and adverse health effects: Applying Bradford Hill's criteria for causation. Environmental Disease. 2021;**6**:65-87

[6] Zajamsek B, Micic G, Hansen K, Catcheside DPN. Wind farm infrasound detectability and its effects on the perception of wind farm noise amplitude modulation. In: Proceedings of the Annual Conference of the Australian Acoustical Society; 10–13 November 2019. Cape Schanck, Victoria, Australia; 2019. pp. 487-494

[7] Maijala P, Turunen A, Kurki I, Vainio L, Pakarinen S, et al. Infrasound Does Not Explain Symptoms Related to Wind Turbines. Helsinki, Finland: Publication Series of the Government's Study and Research Activities; 2020. p. 34

[8] Ratzel U, Bayer O Brachat P, Hoffmann M, Janke K et al. Low frequency noise including infrasound from wind turbines and other sources: Report on results of the measurement project 2013-2015. State Office for the Environment, Measurement and Nature Conservation of the Federal State of Baden-Wuerttemberg, Karlsruhe, Germany. 2020. https://pudi.lubw.de/detailseite/-/publication/13796-Report_on_results_of_the_measurement_project_2013-2015.pdf

[9] Crichton F, Chapman S, Cundy T, Petrie KJ. The link between health complaints and wind turbines: Support for the nocebo expectations hypothesis. Frontiers of Public Health. 2014;**2**: Article 220

[10] Pedersen E, van den Berg F, Bakker R, Bouma J. Response to noise from modern wind farms in The Netherlands. Journal of the Acoustical Society of America. 2009;**126**:634-643. DOI: 10.1121/1.3160293

[11] Agnew RCN, Smith VJ, Fowkes RC. Wind turbines cause chronic stress in badgers (meles meles) in Great Britain. Journal of Wildlife Diseases. 2016;**53**: 459-467

[12] Zou LH, Shi YJ, He H, Jiang SM, Huo FF, et al. Effects of FGF2/FGFR1 pathway on expression of A1 astrocytes after infrasound exposure. Frontiers in Neuroscience. 2019;**13**:429. DOI: 10.3389/fnins.2019.00429

[13] Zhao JH, Wang JH, Luo JY, Guo XY, Wang Y, et al. Effects of infrasound on gastric motility, gastric morphology and expression of nitric oxide synthase in rat. Biomedical and Environmental Sciences. 2018;**31**:399-402. DOI: 10.3967/bes2018.052

[14] ISO1996-2:2007(E). Acoustics. Description, Measurement and

Assessment of Environmental Noise. Part 2: Determination of Environmental Noise Levels. Geneva, Switzerland: ISO; 2007

[15] ISO 7196:1995(E). Acoustics. Frequency-weighting Characteristic for Infrasound Measurements. Geneva, Switzerland: ISO; 1995

[16] Health Protection Agency (UK). Health Effect of Exposure to Ultrasound and Infrasound—Report of the Independent Advisory Group on Non-ionising Radiation. London: Health Protection Agency; 2010

[17] IARO-International Acoustics Research Organization-represents a group of scientists who, collectively, hold over 200 years of scientific experience in the field of infrasound and low frequency noise, and its effects of human health. Since 2016, our researchers have been recording and analysing acoustical data in and near homes located in the vicinity of onshore wind power stations, in the following countries (alphabetical): Australia, Canada, Denmark, England, France, Germany, Ireland, New Zealand, Northern Ireland, Portugal, Scotland, Slovenia, and The Netherlands. Prior to 2016, all IARO scientists were already working either in acoustics alone or in acoustics and health. All research conducted by IARO is part of the Citizen Science Initiative for Acoustic Characterization of Human Environments (CSI-ACHE), the research protocols for which have been approved by the New Zealand Ethics Committee (application number NZEC19_12). www.iaro.org.nz

[18] Bakker HHC, Rapley BI, Summers SR, Alves-Pereira M, Dickinson PJ. An affordable recording instrument for the acoustical characterisation of human environments. In: Proceedings International Conference Biological Effects of Noise (ICBEN). Zurich, Switzerland; 2017

[19] Model No.: EM246 ASSY, Primo Co, Ltd, Tokyo, Japan. Available from: https://www.primo.com.sg/components/

[20] IPMA [Portuguese National Institute for the Sea and Atmosphere]. www.ipma.pt

[21] Open Weather, London, UK, 2022. http://www.openweathermap.org

[22] Weichenberger M, Bauer M, Kuhler R, Hensel J, Forlim CG, et al. Altered cortical and subcorticol connectivity due to infrasound administered near the hearing threshold – Evidence from fMRI. PLoS One. 2017;**12**:e0174420. DOI: 10.1371/journal. pone.0174420

[23] The Mathworks, Natick, USA, v2020b. It should be noted that the Matlab findpeaks function can sometimes return significantly higher prominences than their definition allows. Another method was developed to derive the appropriate prominence level: IARO21-3. White Paper on the Harmonic Prominence Measure. IARO, Palmerston North, New Zealand. Available from: https://iaro.org.nz/wp-content/uploads/2022/01/IARO21-3-White-Paper-on-the-Harmonic-Prominence-Measure-v6.pdf.

[24] World Health Organization. Environmental noise guidelines for the European region. 2018. ISBN 978 92 890 5356 3. Available from: https://www.euro.who.int/en/publications/abstracts/environmental-noise-guidelines-for-the-european-region-2018

[25] Alves-Pereira M, Bakker HHC. Occupational and residential exposures to infrasound and low frequency noise in aerospace professionals: Flawed assumptions, inappropriate quantification of acoustic environments, and the inability to determine dose–response. Scientific Journal of Aerospace Engineering and Mechanics. 2017;**1**(2): 83-98

[26] Alves-Pereira M, Krough C, HHC B, Summers R, Rapley B. Infrasound and low frequency noise guidelines – Antiquated and irrelevant for protecting populations. In: Proceedings of the 26th International Conference on Sound & Vibration. Montreal, Canada; 2019

[27] Alves-Pereira M, Rapley B, Bakker HHC, Summers R. Acoustics and biological structures. In: Abiddine ZE, Ogam E, editors. Acoustics of Materials. London: IntechOpen; 2019